4ICEGE Thessaloniki-GREECE 2007

4th International Conference on
Earthquake Geotechnical Engineering
June 25-28, 2007
Paper No. 1231

THE USE OF ABSORBING BOUNDARIES IN DYNAMIC ANALYSES OF SOIL-STRUCTURE INTERACTION PROBLEMS

Stavroula KONTOE[1], Lidija ZDRAVKOVIC[1], David M. POTTS[1] and Njemile E. SALANDY[2]

ABSTRACT

Two dimensional (2D) plane strain analyses of a large underground structure were employed to compare the performance of three boundary conditions applied at the lateral sides of the mesh. The examined boundary conditions aimed to model the far-field response. To check their adequacy, the response between the structure and the lateral boundaries of the mesh is compared with the free-field response computed with both the one-dimensional site response software EERA, developed by Bardet et al (2000), and with a 1D finite element (FE) model. The first set of analyses computed with the standard viscous boundary of Lysmer and Kuhlemeyer (1969) failed to reproduce the free-field response, while the predicted motion in the vicinity of the structure was seriously damped. The 2D analysis was then repeated using the tied degrees of freedom (TDOF) boundary condition, introduced by Zienkiewicz et al (1988), along the sides of the mesh. It is shown that the TDOF boundary condition can perfectly model the one-dimensional soil response in cases that waves radiating away from the structure towards the boundaries of the mesh are negligible or sufficiently damped. Finally, the last set of analyses employed the Domain Reduction Method of Bielak *et al* (2003) in conjunction with the standard viscous boundary. In this method the seismic excitation is directly introduced into the computational domain and an artificial boundary is needed only to absorb the scattered energy of the system. It is shown that when the DRM is used as a boundary condition the free-field response is recovered away from the structure and the viscous boundary can successfully absorb the scattered energy.

Keywords: *absorbing boundary, free-field, domain reduction.*

INTRODUCTION

One of the major challenges in dynamic analyses of soil-structure interaction problems is to achieve a balance between accurate and economical modelling of the far-field medium. The most common way is to restrict the theoretically infinite computational domain to a finite one introducing artificial boundaries. The reduction of the solution domain makes the computation feasible, but the performance of the artificial boundaries can seriously control the accuracy of the results. The aim of the present study is to highlight common pitfalls in the use of some of these boundaries.

Numerous artificial boundaries have been proposed in the literature over the last 30 years. These can be broadly categorized into three major groups (Kausel and Tassoulas (1981): elementary, local and consistent. Elementary boundaries are the ones commonly used for static analyses (i.e. zero stress or zero displacement boundary conditions) and they thus cannot model the geometrical spreading of energy towards infinity. However they are efficient in cases where the radiation damping is not important, like soft soil – stiff rock interfaces. On the other hand, consistent boundaries (e.g. Lysmer and Waas (1972) and Kausel (1994)) have mathematically complex formulations and satisfy exactly the radiation condition at the artificial boundary. Nevertheless they are rarely used in practice as they are computationally expensive, frequency dependent and their implementation in finite element codes

[1] Imperial College, London
[2] Geotechnical Consulting Group, London

is often problematic. Finally in the case of local boundaries, the radiation condition is satisfied approximately at the artificial boundary, as the solution is local[3] in space and time. Local absorbing boundary conditions are widely used in engineering practice as they provide results in most cases of acceptable accuracy and are far less computationally expensive than the more rigorous consistent boundaries.

The simplest and most widely used local boundary is the standard viscous boundary of Lysmer and Kuhlemeyer (1969). This boundary can be described by two series of dashpots oriented normal and tangential to the boundary of the FE mesh. The great advantage of this approach is that the absorption characteristics are independent of frequency and thus the viscous boundary is suitable for both harmonic and non-harmonic waves. The method is exact only for one-dimensional propagation of body waves, while for two-dimensional and three-dimensional cases perfect absorption is achieved for angles of incidence greater than 30°. In large computational domains waves of extreme angle of incidence are less likely to develop. Hence the performance of the boundary improves significantly the farther it is placed away from the source of excitation or the area of interest (i.e. structure) of the model.

A serious limitation of this approach is that for low frequency excitations it leads to permanent displacements even in elastic systems. Various modifications of the standard viscous boundary have been introduced that overcome this shortcoming: boundaries based on Kelvin elements by Novak *et al* (1978) and Novak and Mitwally (1988), the doubly asymptotic multi-directional boundary of Wolf and Song (1995) and the cone boundary of Kellezi (2000). The physical interpretation of this type of boundary is two series of springs and dashpots oriented normal and tangential to the boundary of the FE mesh. In general the absorbing characteristics of these boundaries are governed by the viscosity components (i.e. dashpots) and they are therefore very similar to those of the standard viscous boundary (Kellezi 1998).

In a number of numerical studies (e.g. Woodward and Griffiths (1996), Brown *et al* (2001), Maheshwari *et al* (2004)) the seismic excitation is applied as an acceleration time history along the bottom mesh boundary located at the soil-rock interface, while the above-mentioned boundaries are applied along the sides of the mesh to model the far field. In the present study such a configuration is used to compare the behaviour of the following boundary conditions:

- The standard viscous boundary (SVB) of Lysmer and Kuhlemeyer (1969)
- The tied degrees of freedom (TDOF) boundary condition (Zienkiewicz *et al*, 1988), which constrains nodes of the same elevation on the two side boundaries to deform identically. This is essentially an elementary boundary condition, which has been reported to perform satisfactorily when waves radiating away from the structure towards the boundaries of the mesh are negligible or sufficiently damped.
- The standard viscous boundary in conjunction with the Domain Reduction Method (DRM) of Bielak *et al* (2003). The DRM is a two-step sub-structuring procedure that was originally developed for seismological applications to reduce the domain that has to be modelled numerically by a change of governing variables. However, the DRM, in conjunction with a conventional absorbing boundary (i.e. the SVB), can also be efficiently used in the numerical modelling of geotechnical earthquake engineering problems as an advanced absorbing boundary condition (Kontoe *et al* (2006)).

Rigorous numerical modelling requires that the width of the FE mesh should be such that free-field conditions (i.e. one-dimensional soil response) occur near to the lateral boundaries of the mesh. Hence to check the adequacy of the examined boundaries, the response between the structure and the lateral boundaries of the mesh is compared with the free-field response computed with both the one-

[3] When a formulation is local (as opposed to a global formulation) in space and time, the solution at a specific boundary degree of freedom only depends on the response of adjacent boundary degrees of freedom at a specific time, or at most, during a limited past period.

dimensional site response software EERA, developed by Bardet *et al* (2000), and with a 1D finite element model. It should be noted that all analyses were performed with geotechnical finite element code ICFEP which has been developed at Imperial College (Potts and Zdravković (1999)).

ANALYSIS DETAILS

General

The present study details a series of 2D dynamic plane strain analyses of the problem illustrated in Figure 1. The arrangement of the analyses is based on a simplified model of a section of the Daikai station in Kobe that collapsed during the 1995 Kobe earthquake in Japan. As the purpose of this study is to compare the performance of the various absorbing boundary conditions applied at the lateral sides of the mesh, the example of the Daikai station was only used to set up the numerical model. The underground structure was wished in place as a rectangular concrete box 17.8m long and 7m high, located at a depth of 5m. The roof slab was 0.8m thick, the invert 0.85m and the side walls 0.9m thick. Three noded beam elements and eight noded quadrilateral solid elements were used to model the structure and the soil respectively. Both the soil and the concrete were modelled as linear elastic materials with 7% Rayleigh[4] damping. The details of the soil stratigraphy and the employed material properties are listed in Table 1. In all the following FE analyses, the time integration was performed with the Generalised-α method (Chung and Hulbert 1993) and with a time step of Δt=0.02sec.

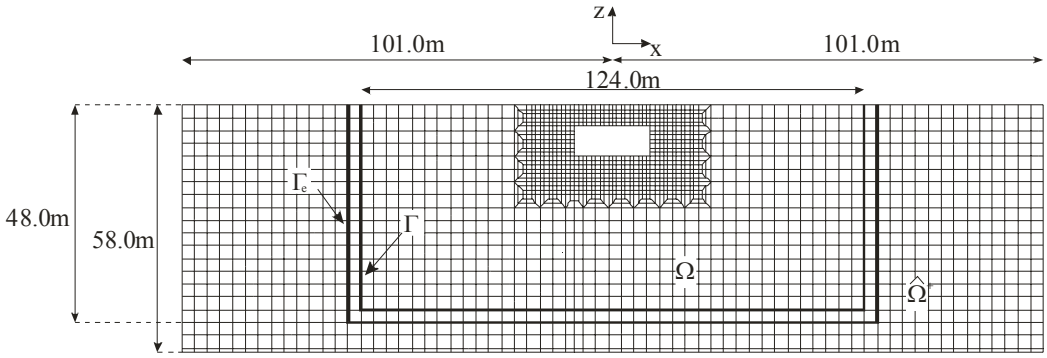

Figure 1: Mesh discretization

Boundary Conditions and Input Ground Motion

In the analyses with the simple boundary conditions (i.e. SVB, TDOF), the excitation was applied along the bottom of the mesh. However in the case of the SVB+ DRM boundary condition the analysis was performed in two steps. In the first step, a 1D model was used to calculate and store the free-field response in terms of effective forces at various depths. In the step I analysis the excitation was applied along the bottom boundary of the 1D model, while the TDOF boundary condition was employed along its lateral boundaries. In the step II analysis, the stored effective forces were applied to the corresponding nodes of the step II 2D model (Figure 1), which are located between the boundaries Γ_e and Γ. This procedure allows the seismic excitation, in the form of equivalent forces calculated in the first step, to be directly introduced into the step II computational domain allowing flexibility in the choice of absorbing boundary conditions. In this study, the SVB was applied along the lateral boundaries of the step II model and both horizontal and vertical displacements were restricted along the bottom boundary. It is important to note that the fictitious boundary Γ separates the computational domain into two areas Ω and $\hat{\Omega}^+$. The formulation of the DRM is such that the perturbation in the external area $\hat{\Omega}^+$ is only outgoing and corresponds to any deviation of the step II 2D model from the step I 1D model. Hence in this study the wave-field in area $\hat{\Omega}^+$ will be solely induced by the presence

[4] The Rayleigh damping coefficients were taken as A=0.524 and B=3.578E-3 resulting in a target damping ratio of 7% for the first two modes of the model.

of the structure. Numerical examples by Yoshimura *et al* (2003) and Kontoe (2006) showed that the ground motion in the external area $\hat{\Omega}^+$ is generally small compared to the corresponding motion of the free-field model. Therefore when the absorbing boundaries are used in conjunction with DRM they are required to absorb less energy than they would have to absorb in a conventional analysis.

The performance of the three above-mentioned boundary conditions (i.e. SVB, TDOF, and SVB+DRM) was compared in two sets of analyses. In the first set of analyses the north-south KJMA acceleration time history (PGA=0.821g) was applied incrementally in the horizontal direction to all nodes along the bottom boundary of the FE models (i.e. SVB, TDOF and 1D), while the corresponding vertical displacements were restricted.

In the second set of analyses both the north-south and the vertical component (PGA=0.34g) of the KJMA record were incrementally applied in the horizontal and vertical directions respectively along the bottom boundary of the FE models. It should be noted that only the significant part of the record (from a time of 4 to 25 seconds) was used in the analyses.

Table 1: Soil stratigraphy and material properties

Material	Thickness (m)	ρ (Mg/m^3)	G (MPa)	v
Fill	3.0	1.96	19.6	0.35
Holocene Clay	3.0	1.8	18.0	0.35
Holocene Sand	3.0	1.9	42.75	0.35
Pleistocene Clay	3.0	1.8	72.0	0.35
Pleistocene Sand	3.0	1.9	109.44	0.35
Pleistocene Clay	3.0	1.8	72.0	0.35
Pleistocene Gravel	40.0	2.0	180.0	0.35
Concrete	-	2.4	24000.0	0.2

ANALYSES RESULTS

Horizontal excitation

As the main focus of this study is to compare the ability of the three boundary conditions to simulate the free-field response in the far field, i.e. at some distance away from the structure, the response at various distances from the axis of symmetry of the 2D FE models (see Figure 1), is compared with the one computed with the 1D models (i.e. FE and EERA).

Figure 2 plots the loci of maximum horizontal acceleration and maximum shear strain with depth computed with the SVB model (at x=10.0m, 40.0, 60.0 and 90.0m), the 1D FE model and EERA for the first set of analyses (i.e. only horizontal excitation). In both plots the 1D FE analysis agrees very well with the solution of EERA. The predicted acceleration and shear strain profiles by the 1D models show a general trend of amplitude attenuation with depth. One would expect the predicted response by the SVB model to match the 1D response for large distances from the axis of symmetry. However, the SVB response is significantly lower than the 1D one for all values of x. It is also interesting to note that the greater is the distance from the axis of symmetry the lower is the SVB response.

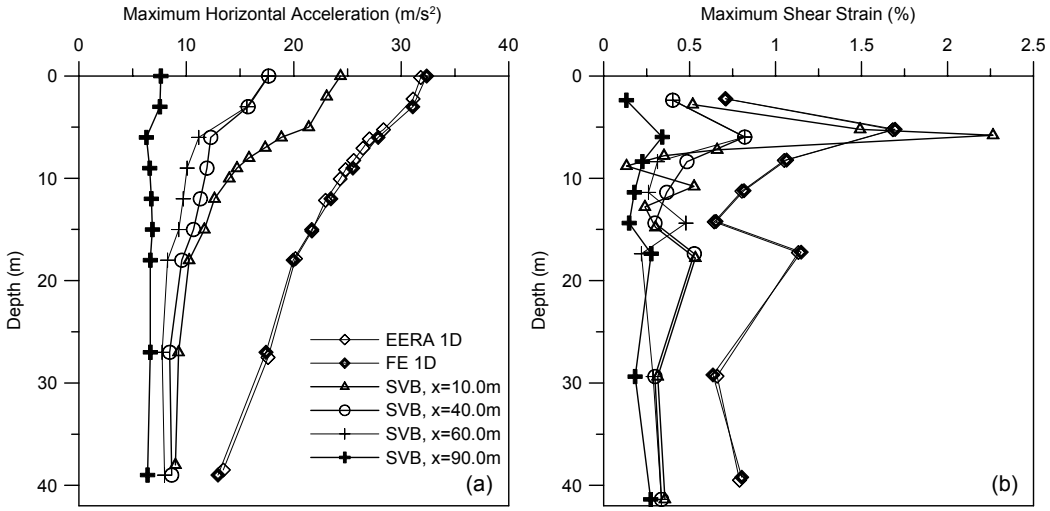

Figure 2: Maximum horizontal acceleration (a) and shear strain profiles (b) computed with the SVB model, the 1D FE model and EERA for the first set of analyses.

Figure 3a shows the acceleration time history at the free surface computed with the 2D SVB model (at x=60.0m and 90.0m), 1D model and EERA and Figure 3b plots the corresponding Fourier spectra. The curves for the 1D FE model and EERA are indistinguishable. This agreement verifies the adopted element discretization in the vertical direction and the choice of the Rayleigh damping coefficients, but it poses serious questions regarding the inability of the SVB analysis to reproduce the free-field response. The predicted response by the SVB is significantly different from the 1D situation both in terms of amplitude and frequency content. These differences become more important close to the lateral boundaries.

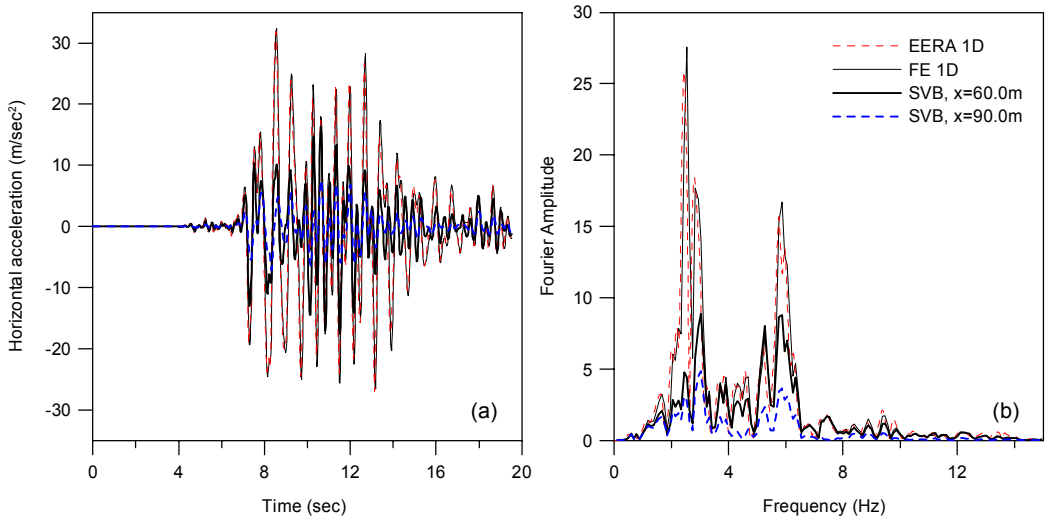

Figure 3: Horizontal acceleration time history (a) and Fourier spectrum (b) at the surface computed with the SVB model, the 1D FE model and EERA for the first set of analyses.

Although similar configurations to the SVB model adopted herein have been widely used in practice, it seems that this model fails to retain the free-field response and it potentially underestimates the response close to the structure. As mentioned above the performance of the SVB usually improves

significantly the farther it is placed away from the source of excitation, as it achieves perfect absorption only for angles of incidence greater than 30°. In the adopted configuration the dashpots were placed very close to the seismic excitation, especially at the bottom corners of the mesh while the shear waves propagate in a direction parallel to the viscous boundary. Therefore, the poor performance of the SVB can be attributed to its misuse.

Figure 4 compares the loci of maximum horizontal acceleration and maximum shear strain with depth predicted by the TDOF model (at x=10.0, 40.0 and 60.0m) with the free-field ones predicted by the 1D FE model for the first set of analyses. The presence of the structure causes some sharp peaks in the shear strain profile and amplification in the acceleration response at x=10m. The structure does not seem to affect the response monitored at x=40.0m and 60.0m. The predicted shear strain profiles at the far-field (i.e. x=40.0m and 60.0m) by the TDOF model are in excellent agreement with the 1D one. In terms of acceleration, the TDOF analysis slightly under-estimates the response close to the surface.

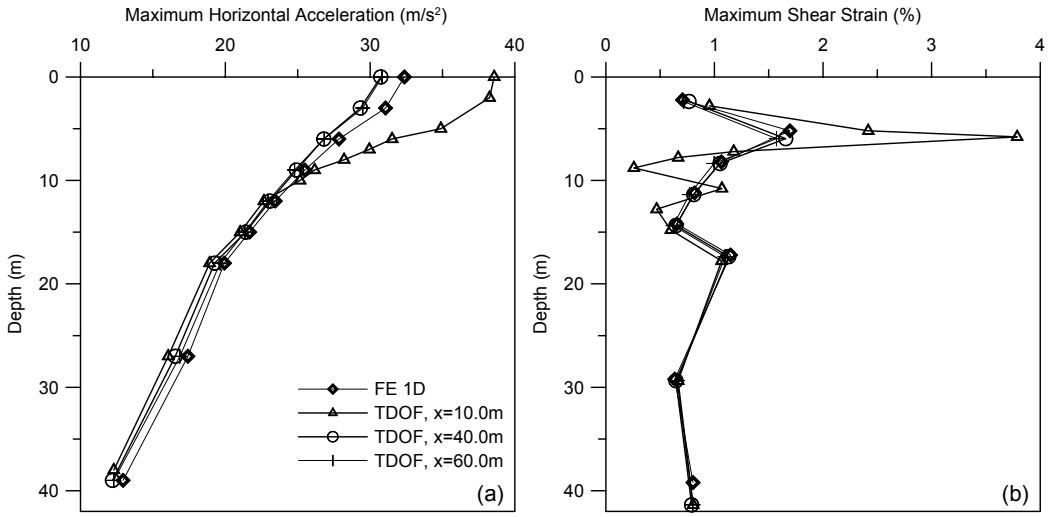

Figure 4: Maximum horizontal acceleration (a) and shear strain profiles (b) computed with the TDOF and 1D FE models for the first set of analyses.

Figure 5 compares the loci of maximum horizontal acceleration and maximum shear strain with depth predicted by the SVB+DRM model (at x=10.0, 40.0 and 60.0m) with the free-field ones predicted by the 1D FE model for the first set of analyses. Generally the SVB+DRM model behaves very similar to the TDOF one (Figure 4). For x=60.0m the acceleration profile computed with the SVB+DRM model is in better agreement with the 1D model than the one computed with the TDOF model.

The excellent performance of the SVB+DRM model verifies the earlier speculation that the poor performance of the SVB model is due to the misuse of the viscous boundary. In the SVB+DRM simulation the excitation is introduced into the mesh and the motion in area $\hat{\Omega}^+$ (see Figure 1) is only outgoing, due to reflections from the structure. Hence in the SVB+DRM model the viscous boundary performs well because it is placed away from the excitation and has to absorb less energy.

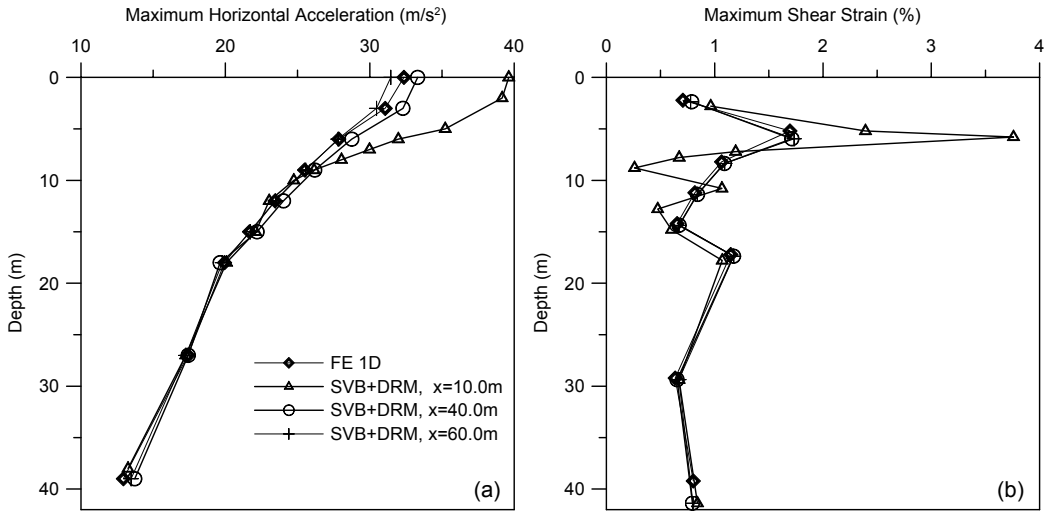

Figure 5: Maximum horizontal acceleration (a) and shear strain profiles (b) computed with the SVB+DRM and 1D FE models for the first set of analyses.

Horizontal and vertical excitation

The numerical results considered so far indicate that the simple TDOF boundary condition is good enough to simulate the far-field response. However, it is difficult to draw such a general conclusion from just one set of analysis. Generally the TDOF boundary can perfectly model the one-dimensional soil response, but it cannot absorb waves radiating away from the structure (or any type of irregularity) and thus it can result in wave-trapping into the mesh. To further investigate this, a second set of analysis was performed subjecting the underground structure to two components of the earthquake motion as described in a previous section. The vertical component of the motion subjects the model to a series of vertically propagating compression waves. It is therefore interesting to investigate whether the TDOF boundary condition performs well in the case of a more complicated wave-field caused by the interaction of compression and shear waves.

Figures 6 and 7 compare the profiles of maximum horizontal and vertical acceleration with depth predicted by the TDOF and the SVB+DRM models respectively (at x=10.0m, 40.0and 60.0m) with the free-field ones predicted by the 1D FE model. As in the first set of analyses, the TDOF and the SVB+DRM models predict a similar far-field response (i.e. x=60.0m) which compares very well with the one-dimensional behaviour. They also predict very similar horizontal acceleration profiles in the near field (x=10.0m). However, the near-field vertical acceleration profiles significantly differ close to the surface. Figure 8 presents the vertical acceleration time histories at the free surface at x=10.0m computed by the TDOF and the SVB+DRM models and the corresponding Fourier spectra. The TDOF without significantly altering the frequency content of the motion seems to considerably damp the vertical response. One explanation for this could be that reflected waves at the lateral sides of the mesh cancel out with outgoing waves from the structure leading to serious underestimation of the response. This is probably why the acceleration time histories predicted by the two models are very similar for the first 4 seconds and then they start to diverge as reflected waves approach the near field area. However such an explanation is not consistent with the observation that this model predicts well the free-field response in the vertical direction. Theoretically the TDOF method gives inaccurate results when the waves radiating away from the structure towards the boundaries of the mesh are not negligible or not sufficiently damped. This is often the case when the geometry of the problem in the near field is significantly different to that of the far-field (e.g. analyses of gravity retaining walls). This second set of analyses suggests that further research is needed to highlight under which conditions it is appropriate to use the TDOF boundary condition.

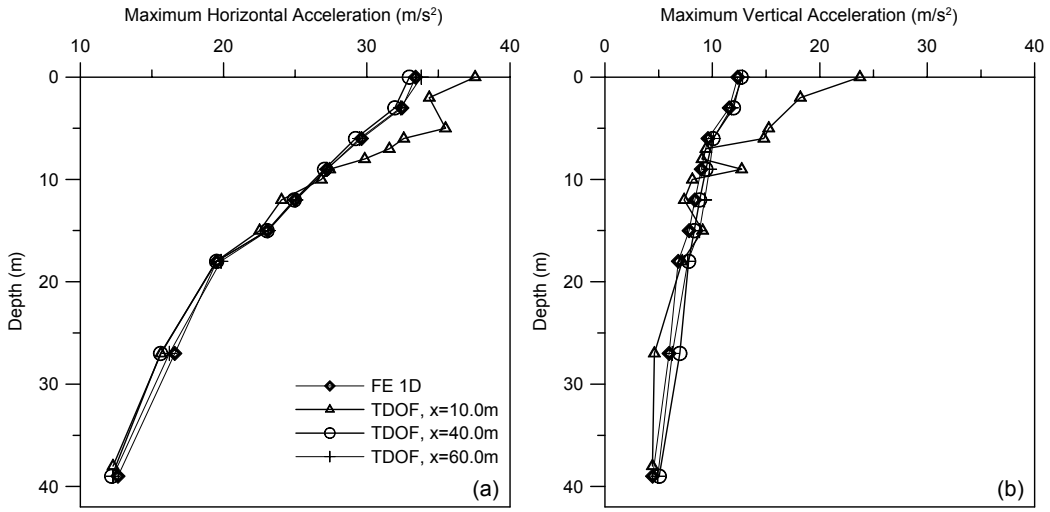

Figure 6: Maximum horizontal (a) and vertical (b) acceleration profiles computed with the TDOF and the 1D FE models for the second set of analyses.

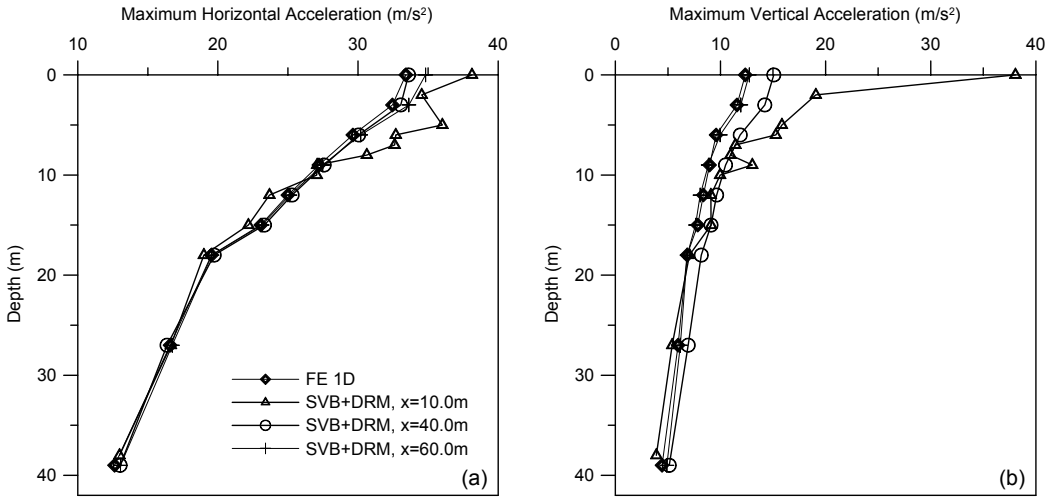

Figure 7: Maximum horizontal (a) and vertical (b) acceleration profiles computed with the SVB+DRM and the 1D FE models for the second set of analyses.

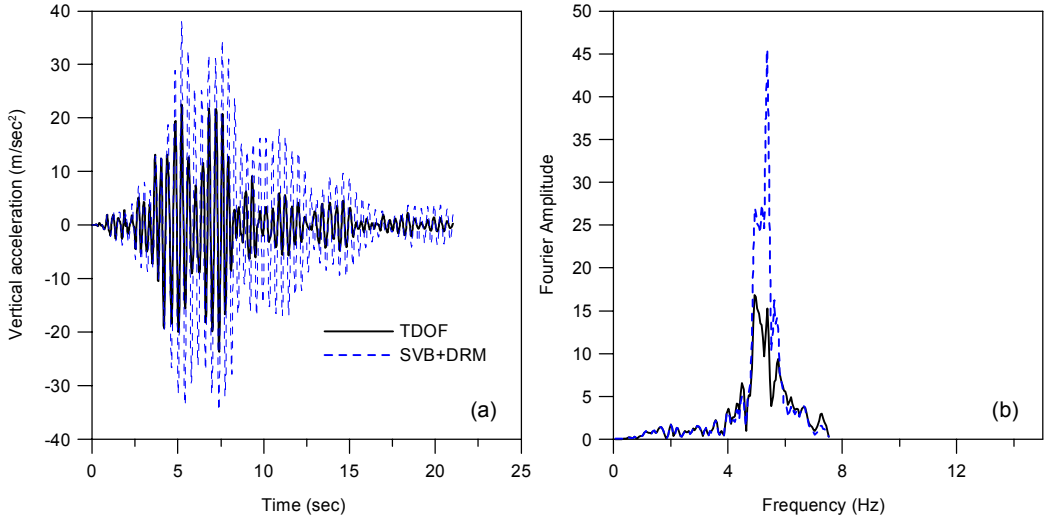

Figure 8: Near field (x=10.0m) vertical acceleration time history (a) and Fourier spectrum (b) at the surface computed with the TDOF and SVB+DRM models for the second set of analyses.

CONCLUSIONS

This paper details the results from two dimensional plane strain dynamic finite element analyses of an underground structure for various boundary conditions imposed at the lateral sides of the mesh. In all cases the excitation was applied at the bottom boundary of the mesh and the artificial boundaries were aiming to simulate the free-field response. Two sets of analyses were performed. In the first one, the FE models were subjected only to a horizontal excitation, while in the second they were simultaneously subjected to both a horizontal and a vertical excitation. To check the adequacy of the examined boundaries (i.e. the standard viscous boundary, the tied degrees of freedom and the standard viscous boundary with the domain reduction method), the response between the structure and the lateral boundaries of the mesh was compared with the free-field one computed with both the one-dimensional site response software EERA and with a finite element 1D model. Several conclusions can be drawn from the results of the present study:

- The SVB model although widely used in engineering practice, failed to reproduce the free-field response and lead to serious underestimation of the response in the near field. Its poor performance can be attributed to the fact that the dashpots were placed very close to the excitation (i.e. bottom boundary of the mesh). It should be noted that this deficiency of the SVB model potentially characterises all boundary conditions consisting of dashpots (e.g. boundaries based on Kelvin elements). Hence these boundaries should be used with caution in earthquake engineering problems.
- Conversely the viscous dashpots performed very well when they were used together with the DRM method. The SVB+DRM model allows the dashpots to be placed at some distance from the excitation. Furthermore, in this case the dashpots have to absorb only the scattered energy from the structure.
- In both sets of analyses the TDOF boundary condition predicted very well the free-field response. However, in the second set of analyses the TDOF model predicted lower response in the near field than the SVB+DRM one. This could be due to superposition of waves "trapped" into the mesh. Overall, the results of this study show that the TDOF can be successfully used in cases where the waves radiating away from the structure towards the boundaries of the mesh are negligible or sufficiently damped. Hence when the geometry of the problem in the near field is significantly different than that of the far-field (e.g. analyses of retaining walls) the use of a TDOF boundary condition can lead to inaccurate results.

APPENDIX

Notation

A, B Parameters used in evaluating the Rayleigh damping matrix.
G: Shear modulus.
Γ: Boundary between the internal (Ω) and the external area (Ω^+) in the domain reduction method.
Γ_e: Boundary within the external area in the domain reduction method defining a strip of elements between Γ_e and Γ.
Δt: Incremental time step.
ν: Poisson's ratio.
ρ: Material density.
Ω: Internal area of both the step I and II models in the domain reduction method.
$\hat{\Omega}^+$: External area of the step II model in the domain reduction method.

REFERENCES

Bardet J.P., Ichii K. & Lin C.H. (2000), "EERA, A computer program for Equivalent linear Earthquake site Response Analysis of layered soils deposits" University of Southern California, Los Angeles.

Bielak J., Loukakis K., Hisada Y. & Yoshimura C. (2003), "Domain Reduction Method for Three-Dimensional Earthquake Modeling in Localized Regions, Part I: Theory", *Bulletin of the Seismological Society of America,* Vol. 93, No 2, pp. 817-824.

Brown D.A., O'Neill M.W., Hoit M., McVay M., El Naggar M.H. & Chakraborty S., (2001), "Static and Dynamic Lateral Loading of Pile Groups", NCHRP report 461, National Academy Press, Washington, D.C.

Chung J. & Hulbert, G.M. (1993), "A time integration algorithm for structural dynamics with improved numerical dissipation: the generalized-α method", *Journal of Applied Mechanics*, Vol. 60, pp. 371–375.

Kausel E. & Tassoulas J. L. (1981), "Transmitting Boundaries: A closed-form comparison", *Bulletin of the Seismological Society of America,* Vol. 71, No 1, pp. 143-159.

Kausel E. (1994), "Thin-layer method: formulation in time domain", *International Journal for Numerical Methods in Engineering*, Vol.37, pp.927-941.

Kellezi L. (2000), "Local transmitting boundaries for transient elastic analysis", *Soil Dynamics and Earthquake Engineering*, Vol.19, pp. 533-547.

Kontoe S. (2006), "Development of time integration schemes and advanced boundary conditions for dynamic geotechnical analysis", PhD thesis, Imperial College, London.

Kontoe S., Zdravković L. & Potts D.M. (2006) "The Domain Reduction Method as an advanced boundary condition" submitted to the *International Journal for Numerical and Analytical Methods in Geomechanics*.

Lysmer J. & Kuhlemeyer R.L. (1969), "Finite dynamic model for infinite media" Journal of the Engineering Mechanics Division, ASCE, Vol.95, No.4, pp. 859-877.

Lysmer J. & Waas G. (1972), "Shear waves in plane infinite structures", *Journal of Engineering Mechanics Division*, ASCE Vol. 98, No. 1, pp.85-105.

Maheshwari B.K., Truman K.Z., El Naggar M.H. & Gould P. L. (2004), "Three-dimensional finite element nonlinear dynamic analysis of pile groups for lateral transient and seismic excitations" *Canadian Geotechnical Journal*, Vol. 41, pp. 118-133.

Novak M. & Mitwally H. (1988), "Transmitting boundary for axisymmetric dilation problems", *Journal of Engineering Mechanics Division*, ASCE Vol. 104, No. 4, pp.953-956.

Novak M., Nogami T. & Aboul-Ella F. (1978), "Dynamic so reactions for plane strain case", Technical Note, *Journal of Engineering Mechanics Division*, ASCE, Vol.112, No. 3, pp. 363-368.

Potts D.M. & Zdravković L.T. (1999), *Finite element analysis in geotechnical engineering: theory*, Thomas Telford, London.

Wolf J.P. & Song C. (1995), "Doubly asymptotic multi-directional transmitting boundary for dynamic unbounded medium-structure interaction analysis", *Earthquake Engineering & Structural Dynamics*, Vol.24, pp. 175-188.

Woodward P.K. & Griffiths D.V. (1996), "Comparison of pseudo-static and dynamic behaviour of gravity retaining walls", *Geotechnical and Geological Engineering*, Vol.14, pp. 269-290.

Yoshimura C., Bielak J., Hisada Y. & Fernández A. (2003), "Domain Reduction Method for Three-Dimensional Earthquake Modeling in Localized Regions, Part II: Verification and Applications", *Bulletin of the Seismological Society of America,* Vol. 93, No 2, pp. 825-840.

Zienkiewicz O.C., Bianic N. & Shen F.Q. (1988), "Earthquake input definition and the transmitting boundary condition", Conf: *Advances in computational non-linear mechanics*, Editor: St. Doltnis I., pp. 109-138.